JACS
JOURNAL OF THE AMERICAN CHEMICAL SOCIETY

ARTICLE

pubs.acs.org/JACS

Light-Induced Conformational Change and Product Release in DNA Repair by (6−4) Photolyase

Masato Kondoh,[†] Kenichi Hitomi,[‡,§] Junpei Yamamoto,[§] Takeshi Todo,[∥] Shigenori Iwai,[§] Elizabeth D. Getzoff,[‡] and Masahide Terazima*[,†]

[†]Department of Chemistry, Graduate School of Science, Kyoto University, Oiwake, Kitashirakawa, Sakyo-ku, Kyoto 606-8502, Japan

[‡]Department of Molecular Biology and The Skaggs Institute for Chemical Biology, The Scripps Research Institute, La Jolla, California 92037, United States

[§]Division of Chemistry, Graduate School of Engineering Science, Osaka University, Toyonaka, Osaka 560-8531, Japan

[∥]Department of Radiation Biology and Medical Genetics, Graduate School of Medicine, Osaka University, Osaka 565-0871, Japan

Supporting Information

ABSTRACT: Proteins of the cryptochrome/photolyase family share high sequence similarities, common folds, and the flavin adenine dinucleotide (FAD) cofactor, but exhibit diverse physiological functions. Mammalian cryptochromes are essential regulatory components of the 24 h circadian clock, whereas (6−4) photolyases recognize and repair UV-induced DNA damage by using light energy absorbed by FAD. Despite increasing knowledge about physiological functions from genetic analyses, the molecular mechanisms and conformational dynamics involved in clock signaling and DNA repair remain poorly understood. The (6−4) photolyase, which has strikingly high similarity to human clock cryptochromes, is a prototypic biological system to study conformational dynamics of cryptochrome/photolyase family proteins. The entire light-dependent DNA repair process for (6−4) photolyase can be reproduced in a simple *in vitro* system. To decipher pivotal reactions of the common FAD cofactor, we accomplished time-resolved measurements of radical formation, diffusion, and protein conformational changes during light-dependent repair by full-length (6−4) photolyase on DNA carrying a single UV-induced damage. The (6−4) photolyase by itself showed significant volume changes after blue-light activation, indicating protein conformational changes distant from the flavin cofactor. A drastic diffusion change was observed only in the presence of both (6−4) photolyase and damaged DNA, and not for (6−4) photolyase alone or with undamaged DNA. Thus, we propose that this diffusion change reflects the rapid (50 μs time constant) dissociation of the protein from the repaired DNA product. Conformational changes with such fast turnover would likely enable DNA repair photolyases to access the entire genome in cells.

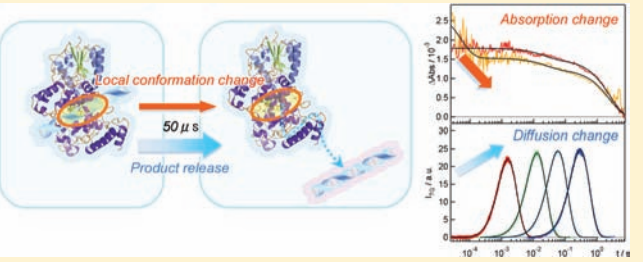

INTRODUCTION

Light is essential for life, yet ultraviolet (UV) light can be harmful due to its damaging photochemical reactions with biological molecules. For example, UV-induced chemical reactions between two adjacent pyrimidine bases within the same DNA strand produce two major photoproducts:[1] 70−80% are cyclobutane pyrimidine dimers (CPDs) and 20−30% are pyrimidine−pyrimidone (6−4) photoproducts ((6−4) PPs) (Figure 1). To maintain genetic integrity, organisms use self-defense machineries. Photolyases (PHR) are unique DNA repair enzymes, which light-dependently catalyze the conversion of these photoproducts to original pyrimidines.[2,3] Two types of PHRs are known: CPD photolyase (CPD PHR), which repairs only CPDs, and (6−4) photolyase ((6−4) PHR), which recognizes and repairs (6−4) PPs and some isomers. Besides these PHRs, many higher organisms have PHR-like proteins termed cryptochromes (CRYs), controlling growth and flowering in plant and daily rhythms in animals.[4] The PHRs and CRYs have a common choromophore, flavin adenine dinucleotide (FAD). Within the cryptochrome/photolyase family, the (6−4) PHRs show the highest sequence and structural similarities to mammalian circadian clock-related CRYs.[5]

The intriguing light-dependent DNA repair catalyzed by PHRs has been the subject of many biochemical, biophysical, and spectroscopic studies to date.[4−19] PHRs first recognize damage and form a stable complex with their substrates in the dark. Regardless of substrate specificity, fully reduced FAD ($FADH^-$) is the catalytically active form for both CPD and (6−4) PHRs,[6,7] while PHRs with oxidized FAD are completely inactive (Figure 2). Accordingly, it has been proposed that the catalytic reaction for CPD PHR is initiated by an electron transfer

Received: August 26, 2010
Published: January 27, 2011

   dx.doi.org/10.1021/ja107691w | J. Am. Chem. Soc. 2011, 133, 2183–2191

from the excited $FADH^-$ to the damaged site in DNA, resulting in bond breakage within the dimers and formation of the transient radical $FADH^{\cdot}$. The redundant electron in the DNA returns to the FAD to restore the original species ($FADH^-$) after DNA repair.[3,4]

CPD and (6−4) PHRs share not only the same cofactor but also a common fold. Therefore, properties of (6−4) PHR have been estimated by analogy with the well-characterized CPD PHRs derived from bacteria.[4,7−10] However, (6−4) PP has a more complicated structure than does CPD (Figure 1), implying that the repair mechanism for (6−4) PHR is also more complex. Yet, the detailed repair mechanim remains debatable due to a lack of enough information on transition states. Two distinguished models have been proposed for the repair of (6−4) PP, which consists of two linked thymidines. The transient water molecule formation model proposes direct breakage of the C−O bond at the 5′ base after the initial proton transfer,[11] whereas the transient four-membered ring formation model implies the formation of a simple oxetane ring (Figure 1) facilitates the oxygen-atom transfer from the 5′ to 3′ base followed by the C6−C4 bond split.[12,13] In addition to repairing thymidine−thymidine (6−4) PP, (6−4) PHR also repairs thymidine−cytidine (6−4) PP by an amino group instead of a hydroxyl group with no siginificant mutagenic side effects,[14] making the four-membered ring formation model more attractive. Regardless of the exact mechanism, an active site histidine (His354 in *Xenopus* (6−4) PHR) is essential for the repair.[15] DNA mobility shift data showed the formation of the stable complex between PHR and the substrate in the dark.[6,16] Most studies on (6−4) PHR have focused on local conformational changes, yet little is known about the dynamics of overall PHR−DNA interactions during the repair

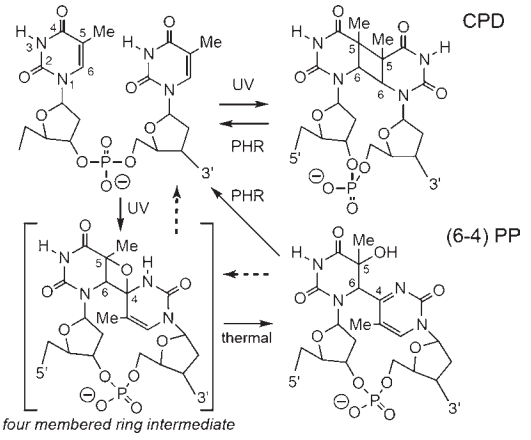

Figure 1. The structures of cyclobutane pyrimidine dimers (CPD) and (6−4) photoproducts ((6−4) PP) between neighboring thymines. The structure of the four-membered ring intermediate was also shown. PHRs convert the photoproducts to restore original thymines (solid arrows). The dashed arrows show one of the proposed repair reaction paths by (6−4) PHR.[12]

reaction in solution. A recent ultrafast experiment excluded the existence of the stable four-membered ring intermediate in the dark and revealed the initial electron transfer and the subsequent proton transfer reactions from the enzyme to the bases near the active site to form the proposed transient oxetane intermediate with rates on the order of hundreds of picoseconds.[12] However, the dynamics of (6−4) PHR in a longer time range that includes its dissociation from DNA after the light-dependent repair are still unclear.

To date, many studies on photoreceptors have been done by ultraviolet/visible (UV/vis) light detection methods using the characteristic absorption of cofactors. Generally, those experiments report on local interactions between the protein and cofactor, but provide very little information regarding global protein or intermolecular interactions. Because the reported crystal structures of PHR showed that the substrate binding site is close to the chromophore both in the CPD[8] and in the (6−4) PHR,[11,17−19] UV/vis absorption methods, which are sensitive to reactions around the chromophore, have been important for understanding the repair mechanism of PHR. However, in addition to the chromophore reaction, protein conformational changes distant from the chromophore should be essential, because PHR has to bind with and transfer electrons to the (6−4) PP substrate buried inside the DNA duplex, and, after the repair, the product (restored DNA) has to dissociate from PHR to initiate a new reaction cycle with another substrate molecule. Therefore, to better understand the PHR reaction mechanism, it is essential to capture multiple stages in the DNA repair process, from damage recognition to product release with time-resolved methods. Furthermore, we believe that studies on (6−4) PHR will provide fundamental insights into the roles of mammalian CRYs in the circadian clock. Lack of methods for detecting both entire protein dynamics and cofactor redox status simultaneously prevented us from studying this previously. However, a new method exists (described below), which has allowed our recent undertaking of these studies.

To observe time-resolved dynamics of DNA repair by (6−4) PHR in solution, we have applied the transient absorption (TA: absorption), transient lens (TrL: absorption and volume), and transient grating (TG: absorption, volume, and diffusion) techniques to the full-length (6−4) PHR reaction, and then we integrated all the results from these complementary techniques with existing knowledge. The TA method allows us to detect the redox state of chromophores simply through the changes in the optical absorption spectra, which is suitable for monitoring interaction dynamics in the vicinity of the chromophore, such as electron transfer between PHR and DNA. On the other hand, the TrL and TG methods detect conformational changes that are not characterized by changes in absorption spectra. Furthermore, the TG method is a powerful tool to detect, with high time resolution, changes in the molecular diffusion coefficient (D) during chemical reactions. Therefore, the TG method has been developed as an ideal technique to detect the detailed time

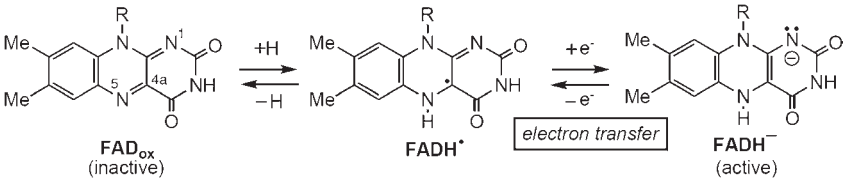

Figure 2. The structure of the flavin chromophore in various redox states.

dependence of intermolecular interactions[20−23] and has been applied to studies, for example, on the dynamics for heterogeneous protein−protein interactions[24] or homogeneous oligomerization.[25]

The studies reported here reveal the DNA repair process of (6−4) PHR, from the initial flavin radical formation to product dissociation. Photoexcitation of (6−4) PHR with fully reduced FAD leads to transient FAD radical formation. In the presence of substrate, the UV absorption of this radical is decreased on a fast time scale, indicating a rapid back electron transfer from the repaired DNA to restore PHR. Remarkably, we also detected a TG signal reflecting a change in the molecular diffusion coefficient only in the presence of substrate, therefore associating this signal with the repair process. We concluded that this signal would likely arise from local conformational changes associated with the dissociation of restored DNA product from the (6−4) PHR. Detailed analysis revealed that this dissociation reaction had a time constant of ∼50 μs. Unlike other DNA repair machineries, such as base excision repair and nucleotide excision repair, consisting of multiple proteins,[26] DNA repair by PHRs is thought to be done alone. Rapid dissociation from DNA after the repair would enable (6−4) PHR enzymes to seek and initiate repair at another damaged site within the enormous DNA contents more efficiently than for other machineries.

EXPERIMENTAL SECTION

Sample Preparation. *Xenopus laevis* full-length (6−4) PHR was prepared as described in previous reports.[6,27] As a substrate, a 14 base pair DNA duplex, which contained a (6−4) PP on a single strand, was used (damaged DNA). For a negative control, we used a 14-mer normal oligonuceotide with the same sequence as damaged DNA (undamaged DNA). Samples were dissolved in the buffer solution containing 50 mM Tris-HCl (pH 8.0), 250 mM NaCl, 50 mM dithiothreitol (DTT), and 5% (v/v) glycerol. Before all the spectroscopic measurements, (6−4) PHR was converted to the fully reduced form as described in the Supporting Information S-1 Materials and Methods section. Additional details can also be found in the Supporting Information S-1 Materials and Methods section.

Measurements. The experimental setup followed conditions similar to those of previous reports.[24,28−32] A laser pulse from the third harmonic of Nd:YAG laser (10 ns pulse width) was used as an excitation beam for all laser experiments to excite the reduced form of (6−4) PHR. Additional details are available in the Supporting Information S-1 Materials and Methods section.

RESULTS

Photoreaction Dynamics of (6−4) Photolyase in the Vicinity of the Chromophore. Figure 3a depicts the transient absorption (TA) spectra for full-length (6−4) photolyase with reduced FAD (PHR_{red}), at three time points following photoexcitation at 355 nm. The enhanced absorption peak in the wavelength range from 500 to 700 nm matches the reported UV/vis absorption for the neutral flavin radical $FADH^{\cdot}$ (Figure 3a, pink curve[33]). These spectra indicate that radical formation ($PHR^{\cdot}$) occurs upon photoexcitation of the protein alone, in the absence of DNA. In the TA spectrum, we also observed a weaker, but significant, absorption change near 449 nm, which is likely derived from light-induced oxidation of PHR_{red}.

Thus, we monitored the time-resolved absorption changes at two different wavelengths 449 and 633 nm (Figure 3b). At 633 nm

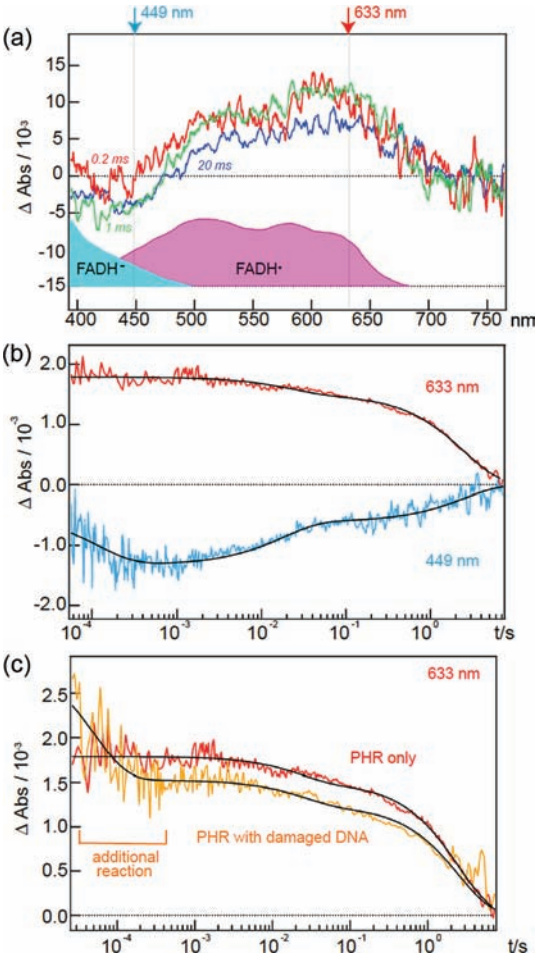

Figure 3. Transient absorption studies identified redox reactions in (6−4) PHR. (a) TA spectra observed after 0.2 ms (red), 1 ms (green), and 20 ms (blue) from photoexcitation of the reduced form of (6−4) PHR (PHR_{red}) at 355 nm showed the enhanced absorption peak in 500−700 nm, indicating the radical formation ($PHR^{\cdot}$) upon photoexcitation of PHR_{red}. Pale blue and pink curves on the figure show absorption spectra of $FADH^{-}$ and $FADH^{\cdot}$, respectively. (b) The time course of the TA signal of (6−4) PHR was monitored at 633 nm (red; $PHR^{\cdot}$ absorption) and 449 nm (blue; PHR_{red} absorption). The signal at 633 nm appeared within a submillisecond, indicating the fast formation of $PHR^{\cdot}$. Both signals decayed to the baseline with the same time scale, indicating these decay components reflected back reaction from $PHR^{\cdot}$ to PHR_{red}. (c) TA signal of the (6−4) PHR + damaged DNA sample (orange) was monitored at 633 nm under exactly the same condition as the measurement of (6−4) PHR (red). By adding substrate, signal intensity in the long time (>1 ms) was decreased by ∼14%. This reflects the decrease of photocreated $PHR^{\cdot}$ by back electron transfer from the repaired DNA, indicating a fast restoration reaction. The 50 μs decay component reflecting the conformational change around the chromophore was also observed. Concentrations of (6−4) PHR and DNA were 120 and 110 μM, respectively.

(red line), the signal appeared within a submillisecond and decayed monotonically to the baseline. In contrast, the signal observed at 449 nm (blue line) gradually increased, then returned to the baseline. The time profile of the 633 nm signal was fitted well by a biexponential function with time constants of 20 ms and 2.5 s, whereas the time profile of the 449 nm signal was reproduced by a three-exponential function with time constants of 120 μs, 20 ms, and 2.5 s. Because the 20 ms and 2.5 s phases

dx.doi.org/10.1021/ja107691w | J. Am. Chem. Soc. 2011, 133, 2183–2191

were observed both for the decay of the PHR$^{\cdot}$ absorption (633 nm) and for dark reversion of PHR_{red} bleaching (449 nm), we assigned these components to the back reaction from PHR$^{\cdot}$ to PHR_{red}. The 120 μs phase was observed uniquely at 449 nm trace. This phase was tentatively assigned to the decay of a transient amino acid radical (see the Supporting Information section S-3, where we described the suggestion for the electron transfer pathway after photoexcitation of PHR_{red}).

Next, we used time-resolved absorption change measurements at 633 nm (Figure 3c) to compare radical formation in the presence and absence of damaged DNA carrying a single (6−4) photoproduct ((6−4) PP). Because the absorption at 633 nm corresponds to the FADH$^{\cdot}$ absorption, the change in the signals should reflect changes in FADH$^{\cdot}$ formation or in its protein surroundings upon the addition of substrate. At longer times (>1 ms), the overall profile of (6−4) PHR with the substrate (orange line) resembled that of (6−4) PHR alone (red line), but with slightly lesser intensity. However, at shorter times (<100 μs), there is an additional fast decay phase. This TA signal for PHR with substrate was reproduced by a three-exponential function with time constants of 50 μs, 20 ms, and 2.5 s. The longer time constants 20 ms and 2.5 s matched those from the protein alone. It should be noted that the decrease in the intensity longer than milliseconds resulting from substrate addition was calculated to be 14%, which is comparable to the reported quantum yield of the light-induced repair reaction (11%).[6] During photorestoration, light-induced conversion of PHR_{red} to the radical PHR$^{\cdot}$ occurs by electron transfer to the substrate, but is reversed by electron transfer back from the restored DNA. Therefore, the decrease in the absorption intensity likely reflects the decrease in PHR$^{\cdot}$ resulting from the repair reaction. Although it is tempting to consider that the 50 μs phase reflects substrate repair, the amplitude of this decay component (ca. 45%) is much larger than the repair efficiency. Notably, the absorption spectrum and absorption coefficient of a chromophore depend on the environment of FAD, that is, protein conformation around the chromophore. If the FADH$^{\cdot}$ environment of protein in complex with the damaged DNA is different from that of protein alone or with the undamaged DNA, the intensity of the absorption changes could be also different among these samples. Thus, we consider that this 50 μs phase likely reflects the process of changing the protein conformation from the repair mode to its original ground-state conformation. We will discuss this fast phase in more detail below.

Photoreaction Dynamics of (6−4) Photolyase Apart from the Chromophore. The absorption spectrum changes monitored by TA reflect chromophore reactions and nearby protein conformational changes. To detect protein conformation changes distant from the chromophore, we used transient lens (TrL) and transient grating (TG) techniques to monitor spectrally silent protein dynamics. Both methods can detect changes in refractive index (δn), which reflect changes in various properties, including absorption, volume, and temperature. The principles and advantages of TrL and TG are described in the Supporting Information S-2 Principles section. Here, we describe results from the TrL measurements (Figure 4) on full-length (6−4) PHR, as compared to those from the calorimetric reference sample bromocresol purple (BCP). BCP promptly releases the excited-state energy as thermal energy, so the TrL signal of BCP consists purely of the thermal lens component. The decay of the TrL signal represents thermal diffusion from the photoilluminated region. If (6−4) PHR exhibits no conformation

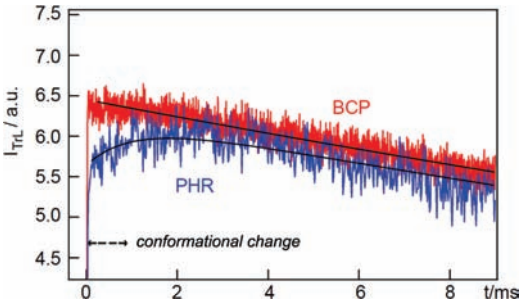

Figure 4. The transient lens method outlines the light-induced conformation change in (6−4) PHR. TrL signals after photoexcitation of (6−4) PHR (blue) and calorimetric reference sample BCP (red) were measured. In the reference sample, only the decay process of thermal lens component was observed. In the (6−4) PHR sample, an additional rise component (~1 ms) appeared on the thermal lens signal. Note these kinetics were not observed in the TA measurement. This indicates the reaction dynamics reflecting the volume change of (6−4) PHR.

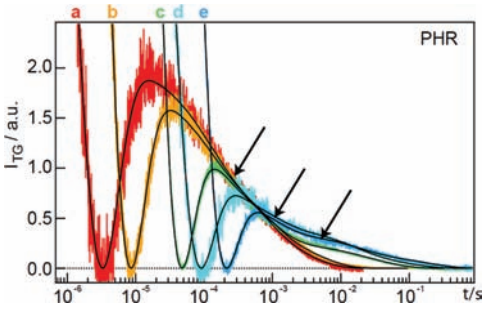

Figure 5. Photoreaction and diffusion dynamics of (6−4) PHR was observed by the transient grating method. TG signals of (6−4) PHR were observed at q^2 of (a) 286, (b) 133, (c) 26.7, (d) 12.4, and (e) 6.68×10^{10} m^{-2}. The best fitted curves are shown by the black lines. Note that some phases (arrows) were observed without depending on q^2. These phases reflect the reaction dynamics observed also in TA and TrL measurements. On the other hand, the time scale of the last decay of each signal depended on q^2, indicating this phase was the diffusion component. The weak decay feature of the diffusion signal indicates there is no D-change in the photoreaction of (6−4) PHR.

change in this time range (besides the temperature increase due to the relaxation from the excited state), the signal of (6−4) PHR should match that of BCP. Instead, we observed a considerable slowly rising component in the TrL signal. The time constant of this rise component was determined to be 1 ms by the fitting of a single exponential component convoluted with the thermal diffusion component. Because this phase was not observed in the TA signal, this 1 ms signal represents the volume change induced by conformation rearrangement of (6−4) PHR distant from the chromophore.

Photoreaction and Diffusion Dynamics of (6−4) Photolyase. For investigating faster, spectrally silent dynamics, we used the TG method, which possesses a time resolution much faster than that of TrL, which is inherently rather slow (~0.5 ms time resolution under present experimental conditions). Furthermore, the TG method has a unique advantage over the other spectroscopy; that is, it can detect the diffusion change in time domain as shown below. Figure 5 shows the TG signals after the photoexcitaion of the full-length (6−4) PHR at various grating wavenumber q^2 (for definition, see the Supporting Information S-2 Principles section) from 6.68×10^{10} to 2.86×10^{12} m^{-2}.

dx.doi.org/10.1021/ja107691w |J. Am. Chem. Soc. 2011, 133, 2183–2191

The TG signal rose with a time resolution of our apparatus (~20 ns), decayed to the baseline once, and then showed a rise and decay profile. The q^2-dependence method allows assignment of these dynamics: rates dependent on the q^2-value represent diffusion processes, whereas rates independent of q^2 should be attributed to reaction kinetics. (The changes in q^2 represent the changes in the spatial dimension of the grating interval, that is, the length for the molecular diffusion.) We found that the rate of the initial decay−rise profile depended on q^2 and its rate constant agreed well with the thermal diffusion rate $D_{th}q^2$, which was determined independently from the calorimetric reference sample, BCP, under the same condition. Hence, this initial large decay−rise component was clearly assigned to the decay process of the thermal grating by thermal diffusion.

After this thermal grating component, the signal decayed in a 100 μs to 1 s time range depending on q^2. By a careful examination of the signal, it was found that the decay profile can be expressed by a combination of q^2-independent and q^2-dependent phases. The q^2-independent phases observed in 10 μs to 10 ms represent reaction dynamics of (6−4) PHR, which should include the kinetics observed by the TA and TrL methods. Nevertheless, the decay rate of the last phase was clearly dependent on q^2, indicating molecular diffusion processes of (6−4) PHR. The weak decay of this signal indicated a single diffusion component. Thus, the molecular diffusion coefficient (D-value) for the protein is the same before (reactant) and after (product) light excitation.

A careful examination of the signal and theoretical considerations (see Supporting Information S-2 Principles) showed that the TG signal for the entire time region should be fitted by a sum of five-exponential functions.

$$I_{TG} = \alpha[\delta n_{th} \exp(-D_{th}q^2t) + a_1 \exp(-(Dq^2+k_1)t) + a_2 \exp(-(Dq^2+k_2)t) + a_3 \exp(-(Dq^2+k_3)t) + a_4 \exp(-Dq^2t)]^2 \quad (1)$$

The signal was reproduced consistently with the time constants previously determined by the TA and TrL methods: k_1^{-1} = 120 μs, k_2^{-1} = 1 ms, and k_3^{-1} = 20 ms. The only variable was the D-value of (6−4) PHR, which was determined to be 3.9(±0.4) × 10^{-11} m^2 s^{-1}. The D-value in aqueous solution was calculated to be 4.6(±0.5) × 10^{-11} m^2 s^{-1} by multiplying the D-value in buffer by the ratio (η/η_0) of the viscosities of the buffer (η) and water (η_0), according to the Stokes−Einstein relationship. This D-value is similar to those of proteins with a comparable size: for example, 4.1 × 10^{-11} m^2 s^{-1} for digestive chymotrypsin (64.5 kDa), 5.3 × 10^{-11} m^2 s^{-1} for G-ADP actin (57.9 kDa), or 5.2 × 10^{-11} m^2 s^{-1} for β-lactamase penicillinase (56 kDa).[34]

Dynamics of the (6−4) Photolyase in Light-Dependent DNA Repair. To gain deeper insights into the DNA repair mechanisms of (6−4) PHR, we applied the TG method to the light-dependent repair reaction of the full-length (6−4) PHR (Figure 6). To extract the DNA repair process from the TG signal, we measured the signal of (6−4) PHR alone, and then in the presence of a DNA oligonucleotide with or without a single (6−4) PP. Adding undamaged DNA did not affect the overall TG profile of (6−4) PHR alone (red and blue lines in Figure 6a). Remarkably, however, the TG profile for (6−4) PHR changed drastically upon addition of damaged DNA carrying (6−4) PP

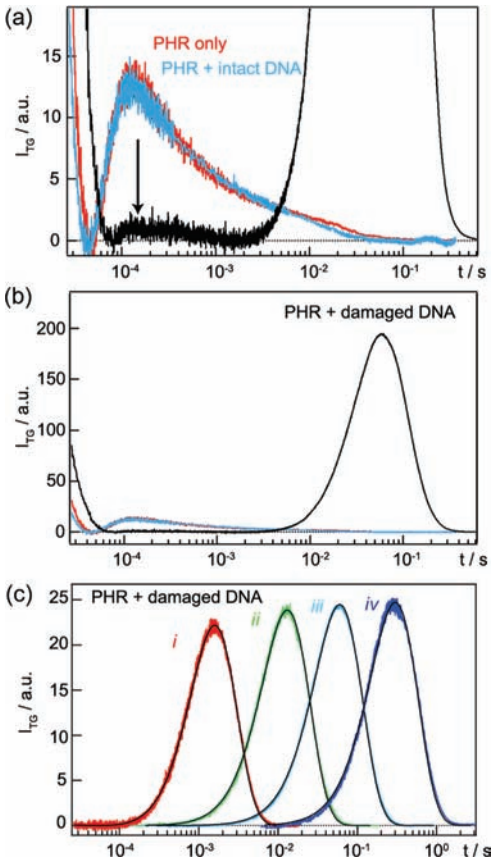

Figure 6. Observation of the light-induced DNA repair of (6−4) PHR by the transient grating method. (a,b) TG signals of (6−4) PHR (red), with intact DNA (blue), and with damaged DNA (black), were measured at q^2 = 3.20 × 10^{11} m^{-2}. The longitudinal axis range was expanded in (b). (c) TG signals of (6−4) PHR with damaged DNA sample were observed at various q^2. The q^2-values are (i) 1030, (ii) 111, (iii) 24.5, and (iv) 4.80 × 10^{10} m^{-2}. From its q^2-dependence, the characteristic rise−decay signal was diffusion signal. The rise−decay feature of the diffusion signal indicates D-change reaction is taking place in the photorestoration reaction of (6−4) PHR. The best fitted curves by eq 2 are shown by the black lines. Concentrations of (6−4) PHR and intact/damaged DNA were 80 and 70 μM, respectively.

(Figure 6b, black line). The initial signal decayed to the baseline, then showed a very small rise−decay feature followed by a strong rise−decay peak. The small rise−decay feature aligns with the peak of (6−4) PHR alone (Figure 6a), whereas the large rise−decay peak is unique for (6−4) PHR with the damaged DNA.

By measuring the signal of (6−4) PHR with the damaged DNA at various q^2 (Figure 6c), we found that the time range of the large rise−decay peak depends on q^2, and thus this signal represents diffusion of (6−4) PHR. The rise−decay feature of this diffusion signal must result from two different diffusion components having opposite signs of light-induced refractive index change, δn. In other words, during the photoreaction of (6−4) PHR with the damaged DNA, there are at least two different species with different molecular diffusion coefficients. Because the sign of the thermal grating δn_{th} is negative at this temperature, we can determine the signs of δn for the rise and decay components to be positive and negative, respectively. Thus, from eq S3, the rise and decay represent the diffusions of product and reactant, respectively.

dx.doi.org/10.1021/ja107691w |J. Am. Chem. Soc. 2011, 133, 2183–2191

Scheme 1

$$PHR:daDNA \xrightarrow{h\nu} (PHR:unDNA)_I \xrightarrow{k} (PHR:unDNA)_P$$

Scheme 2

$$PHR:daDNA \xrightarrow{h\nu} PHR:unDNA \xrightarrow{k} PHR + unDNA$$

The signals at various q^2 (Figure 6c) can be compared by normalizing the intensity for the thermal grating signal from the calorimetric reference sample under the same condition. Following normalization, the signal intensity was almost constant at small q^2 in the long time region. In contrast, the signal intensity slightly decreased at the largest q^2 in the fast time region, indicating changes in the diffusion coefficient occurring at fast times. (Further support is seen in the q^2t plot of the TG signals (Figure S1).) Therefore, we analyzed this q^2-dependence of the signal based on the concept of time-dependent D (described in Supporting Information S-2 Principles section).

Following normalization, the intensity of rise−decay diffusion signals was constant in the relatively small q^2 region (Figure 6c, green and blue), indicating completion of D-change reaction at this longer time. Therefore, the rise−decay feature should be reproduced by a biexponential function in this time region (eq S3). Indeed, the TG signal was reproduced well by this equation, allowing determination of diffusion coefficients for the product ($D_P = 1.0 \times 10^{-10}$ m^2 s^{-1}) and the reactant ($D_R = 4.3 \times 10^{-11}$ m^2 s^{-1}) from this fitting. After viscosity correction, the D-values in aqueous solution are $D_P = 1.1 \times 10^{-10}$ m^2 s^{-1} and $D_R = 4.9 \times 10^{-11}$ m^2 s^{-1}, respectively. This D_R value for (6−4) PHR during the repair is almost identical to the experimentally determined D-value for (6−4) PHR alone ($4.6(\pm0.5) \times 10^{-11}$ m^2 s^{-1}), as determined in the previous section. Therefore, we assigned D_R to D of (6−4) PHR.

Kinetics and Origin of Diffusion Changes in (6−4) Photolyase during DNA Repair. Full-length (6−4) PHR shows a significant D-change only in the presence of damaged DNA. As this change was not observed in the protein alone or with undamaged DNA, the D-change likely results from protein−DNA interactions. Next, we investigated the origin of the D-change observed during DNA repair by (6−4) PHR. Two possibilities were considered: the complex conformational change model (Scheme 1), and the product dissociation model (Scheme 2).

In the complex conformational change model (Scheme 1), the observed D-change represents a conformational change in the (6−4) PHR and DNA complex (PHR:DNA) with a rate constant of k. It has been shown in several systems that D can be changed by intermolecular interactions, even when the molecular size remains unchanged by the reaction.[20−24] Here, daDNA and unDNA stand for DNA with and without a single (6−4) PP, respectively. The subscripts I and P were used to distinguish PHR:unDNA complex before and after conformation change, respectively.

In the product dissociation model (Scheme 2), four different species (PHR:daDNA, PHR:unDNA, PHR, and unDNA) are considered to contribute to the TG signals. Some of these species would share D-values, however, because only two diffusion components are observed. According to the Stokes−Einstein equation, the diffusion coefficient is inversely proportional to the radius of the molecule. If we assume that the radius is proportional to the cube root of molecular mass, D-values for three of the four, PHR (60.5 kDa), PHR:daDNA (69 kDa), and PHR:unDNA (69 kDa), are predicted to be nearly identical. Therefore, the two diffusion components are considered to consist of these three and the restored DNA.

From kinetics alone, these two mechanisms are difficult to distinguish. However, the experimentally determined D-values ($D_R = 4.9 \times 10^{-11}$ m^2 s^{-1} and $D_P = 1.1 \times 10^{-10}$ m^2 s^{-1}) provide a clue. The D_P/D_R ratio of 2.2, calculated from these experimental D-values, was compared to D_P/D_R ratios estimated for Schemes 1 and 2. For Scheme 1, the D-values of the product and reactant would differ, as shown in previous studies on other photoreceptor proteins.[20−22] However, the experimental D_P/D_R ratio is too large to be attributed only to conformational changes within the PHR:DNA complex. For Scheme 2, the ratio derived from PHR (60.5 kDa) and DNA (8.5 kDa) is calculated to be 1.9, by again estimating that the radius is proportional to the cube root of the molecular mass. This estimated ratio matches the experimental D_P/D_R ratio. Therefore, we conclude that the product dissociation model (Scheme 2) is appropriate to describe the repair reaction of the (6−4) PHR. This dissociation model is consistent with the low (insignificant) binding affinity for product DNA (undamaged DNA) with PHR.[16]

On the basis of Scheme 2 and eqs S1, S2, and S6 with $D_I = D_{P_1} = D_R$, $D_{P_2} = D_P$, the temporal profile of the TG signal can be given by:

$$I_{TG} = \alpha[\delta n_{th} \exp(-D_{th}q^2t) + \left(\delta n_I - \delta n_{P_1} - \frac{k}{(D_R - D_P)q^2 + k}\delta n_{P_2}\right) \exp -(D_R q^2 + k)t + \frac{k}{(D_R - D_P)q^2 + k}\delta n_{P_2} \exp(-D_P q^2 t) + (\delta n_{P_1} - \delta n_R) \exp(-D_R q^2 t)]^2 \quad (2)$$

where R, I, P_1, and P_2 denote PHR:daDNA, PHR:unDNA, PHR, and unDNA, respectively. We fitted this equation to the observed TG signals at various q^2, with D_P and D_R set to their previously determined values. The adjustable parameters were the refractive index changes δn and the rate constant k. The TG signals were consistently reproduced by using the rate for this dissociation $k^{-1} = 50(\pm10)$ μs.

Experiment with Excess Amount of the Substrate. To further support the above assignments, we performed the experiment again, under conditions with excess damaged DNA as follows (Figure 7). Under the former condition that substrate concentration is smaller than PHR ([PHR]/[DNA] = 80/70 μM), the diffusion peak appeared immediately after irradiating the pulsed excitation laser (Figure 6). However, when excess amount of substrate exists in the system ([PHR]/[DNA] = 80/90 μM), the diffusion peak was not observed initially (for the initial several pulses of the excitation light), and the signal was similar to that of protein alone or without the substrate (Figure 7, black line). However, after successive laser irradiation without stirring the solution (exact number of the shots depended on the concentrations of the substrate and PHR), the diffusion peak appeared gradually (Figure 7, green and blue lines). This observation clearly excludes the complex conformational model (Scheme 1) for the origin of the D-change, because the conformational change

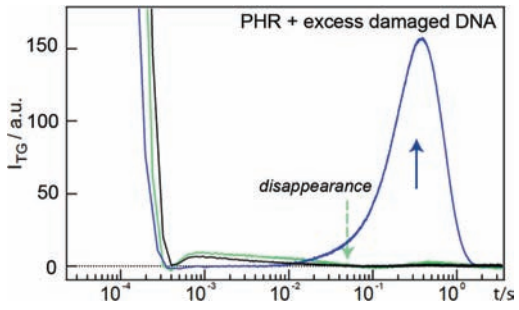

Figure 7. The TG signal of (6−4) PHR with damaged DNA (daDNA) sample was measured under the condition of [PHR] < [daDNA] ([(6−4) PHR] = 80 μM and [daDNA] = 90 μM) at q^2 = 6.49 × 10^{10} m^{-2}. The diffusion signal (the strong rise−decay component) was not observed (black) in this condition. The observation excludes the complex conformational change model (Scheme 1) for the origin of the diffusion change but can be explained in the product dissociation model (Scheme 2). *D*-change reaction coming from dissociation of repaired substrate can be canceled by the subsequent binding reaction between dissociated (6−4) PHR and excess daDNA under this condition. Furthermore, the signal was changed by continuous irradiation of laser pulses without stirring. It gradually appeared by a successive irradiation (after 5 pulses irradiation (green), after 15 pulses irradiation (blue)). Because the successive light irradiation induces the repair reaction in the excitation area and depletes free daDNA, the canceling binding can no longer take place, and then the diffusion signal appeared.

should take place regardless of the substrate concentration. On the other hand, this observation can be explained on the basis of the product dissociation scheme model (Scheme 2) as follows.

Under conditions of [PHR] < [DNA], the solution contained free damaged DNA that awaits repair. This free damaged DNA does not exist under conditions of [PHR] > [DNA] (such as [PHR] ≈ 100 μM) because PHR has a high binding affinity for the damaged DNA (K_D ≈ nM[6]). Under these conditions, by Scheme 2, the following binding reaction occurs as soon as the light-dependent repair reaction yields free protein.

$$\text{PHR} + \text{daDNA} \xrightarrow{k_{on}} \text{PHR :daDNA}$$

Therefore, the overall reaction in the system is

$$\text{PHR :daDNA} + \text{daDNA} \rightarrow \text{PHR :daDNA} + \text{unDNA}$$

In the reaction, the resultant status (PHR:daDNA and unDNA) is indistinguishable from the original status (PHR: daDNA and daDNA) by the diffusion coefficients. The diffusion signals cancel each other out, so that this term does not appear. When we continuously irradiated the sample, however, the repair reaction occurs in this excitation area (~0.8 mm^3), and free damaged DNA is locally depleted. After sufficient light irradiation, [PHR] > [unDNA] at the site of pulsed light irradiation, and the diffusion signal appears.

The above explanation was further confirmed by the following consideration and experiment. In Scheme 2, if this binding rate (k_{on}) is smaller than the molecular diffusion rate (Dq^2), free PHR should diffuse in the solution before binding to the free substrate. If this diffusion occurs, the diffusion signal should appear, even if [PHR] < [daDNA]. Therefore, the appearance of the diffusion peak would depend on the relative magnitude of k_{on} and Dq^2. To examine this effect, we measured the TG signal at a larger q^2 (1.03 × 10^{13} m^{-2}), where the diffusion rate Dq^2 (443 s^{-1}) was sufficiently fast. We found the rise−decay feature appeared without continuous irradiation of pulses at this relatively large q^2 even under a concentration condition of [PHR] < [daDNA] (data not shown). This q^2-dependence strongly indicates association and dissociation takes place within the time of our observations. Although the exact time constant of the binding could not be determined from this experiment, we can roughly estimate k_{on} from the time range of the signal as follows. We found that the rise−decay diffusion signal immediately appeared at around the 10 ms time range at q^2 = 1.03 × 10^{13} m^{-2}, but this signal was absent at the 100 ms time range at q^2 = 6.49 × 10^{10} m^{-2}. Because the appearance of the signal resulted from the competition between k_{on} and the diffusion rate, we calculated approximately that the binding reaction occurred in a time region from 10 to 100 ms. Taking into account that the initial free damaged DNA concentration was ~10−20 μM, we estimate the rate of this binding reaction (k_{on}) is on the order of 10^5 −10^6 M^{-1} s^{-1}. This is consistent with the literature value of k_{on} (k_{on} ≈ 10^5 M^{-1} s^{-1}) at equilibrium.[6]

In this system, the (6−4) PHR might dissociate from the damaged DNA without the repair reaction. However, this possibility is excluded by a prolonged irradiation. We observed that the signal intensity decreased by long-term irradiation of the pulses, indicating that the damaged DNA at the area would be completely repaired. If dissociation occurs without the repair reaction, dissociated damaged DNA can still bind with the (6−4) PHR. In this case, the signal intensity would not significantly decrease. The signal decrease for the long-term irradiation indicates that the dissociated DNA does not bind enzyme again, supporting that the (6−4) PHR releases the restored DNA in the system.

Comparison with the Inactive Mutant of (6−4) Photolyase. To support the observed diffusion change related to DNA repair, we conducted a measurement on a single mutant of the full-length (6−4) PHR. The mutagenesis revealed that two histidines at the active site of (6−4) PHR, which are highly conserved among the (6−4) PHRs but completely missing in CPD PHRs, are essential for the repair *in vitro* and *in vivo* (His354 and His358 of *Xenopus laevis* (6−4) PHR).[15] The H354A mutant of *Xenopus* (6−4) PHR has a high affinity for the substrate, similar to the wild type (WT) enzyme, but completely lacks the activity converting (6−4) PP to normal bases.[15] Thus, H354A forms a relatively stable complex with damaged DNA even under light conditions. We measured the TG signals of the H354A mutant (red line) and WT (black line), respectively, with the damaged DNA under the same condition (Figure 8). In the absence of substrate, the TG signal of H354A was well overlaid with that of WT. There was no significant difference between H354A and WT in the absorption change dynamics and their quantum yield. In the presence of substrate, however, WT and H354A showed different diffusion signals. WT showed the characteristic large rise−decay as described above, whereas H354A did not show a significant signal except for a negligible pseudosignal. This observation supports that the large rise−decay signal for (6−4) PHR in the presence of damaged DNA is derived from the repair and subsequent release of this DNA.

■ DISCUSSION

Light-Induced DNA Repair Mechanism of (6−4) PHR. In this study, we analyzed the entire light-dependent repair process for full-length (6−4) PHR with damaged DNA by using complementary transient spectroscopic techniques. For CPD PHR, Kao *et al.* measured the forward and back electron transfer

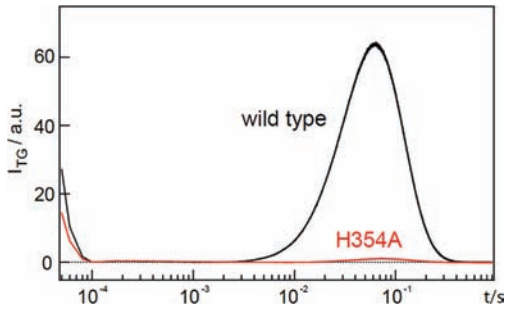

Figure 8. The TG signals of wild-type (6−4) PHR with damaged DNA (black) and H354A mutant with damaged DNA (red) were measured under the same conditions.

between $FADH^-$ and CPDs by an ultra fast absorption technique.[10] They detected the formation and decay of the transient radical $FADH^{\cdot}$ during the repair reaction, which was completed within 1 ns. We discovered that the radical absorption intensity for the (6−4) PHR repair reaction decreased in the presence of the substrate. On a fast time scale, we observed a decay component with the time constant of 50 μs. The amplitude of this component is much larger (45% of the total absorption change) than the restoration efficiency (11%), and its rate, although fast, is much slower than that measured for repair by CPD PHR. Therefore, we do not assign this to the repair reaction. Instead, because we measured product (restored DNA) release from (6−4) PHR with the time constant of 50 μs, the fast phase observed in the TA signal likely reflects the absorption change associated with product dissociation.

The repair of (6−4) PPs includes not only bond cleavage but also transfer of an amino or hydroxyl group, yet the initial essential bond cleavage step is thought to be similar to that for CPD PHRs in the transient four-membered ring formation model;[12] that is, once the four-membered ring is formed, the repair reaction of (6−4) PHR is merely the bond cleavage similar to that of CPD PHR (Figure 1). Because the rate for the formation of the proposed transient oxetane intermediate is reported to be fast (hundreds of picoseconds),[12] we consider the repair reaction by (6−4) PHR is likely completed on the nanosecond time scale such as that by CPD PHR. Also, for the transient water formation model, it was suggested that the restoration of the substrate should be sufficiently fast.[12] If these estimations are correct, (6−4) PHR repairs the damaged DNA first, then releases it much more slowly. This slow rate could result from the conformational changes upon DNA binding to PHR. Because the resulting conformation should favor complex formation, it should also disfavor DNA release by PHR. Therefore, to release the repaired DNA, the PHR:DNA complex should undergo reverse conformational changes near the binding site neighboring the chromophore. Such local conformational rearrangement was also indicated by the crystal structures of the (6−4) PHR:DNA complex before and after repair. The crystal structure of the complex showed that the DNA duplex was fully opened at the damaged site with the (6−4) lesion flipped out almost 180° into the PHR active site.[11] The data also indicated that the hydrogen-bonding contribution from the Gln residue of PHR to the repaired DNA product was smaller than that to the damaged DNA substrate, favoring return of the restored DNA bases into the DNA duplex. The conformational rearrangements required to complete this change are intrinsically slower than the rate for the electron transfer induced bond cleavage reaction. Thus, the complete repair process should involve not only splitting of the lesion to restore the original bases, but also subsequent local conformational changes at the interface between DNA and PHR during dissociation. We propose that such local conformational changes take place on the observed time scale of 50 μs to release the restored DNA. To begin a new restoration cycle after product dissociation, PHR has to seek and bind the new substrate. The binding process after product releasing was estimated to be millisecond time range under our experimental conditions (k_{on} = 10^5-10^6 M^{-1} s^{-1}) as observed in the excess amount of substrate experiment, implying the binding process is rate-limiting step for the repair reaction. To our knowledge, the turnover rate for the repair by (6−4) PHR has not been reported. The turnover rate for the repair by CPD PHR was recently determined to be ∼4 ms (at the substrate concentration of 250 μM), and the rate-determining step of this rate was suggested to be the binding step.[35] This suggestion agrees with our above discussion. However, this binding would be fast enough in a case that the next target (damaged site) is on the same strand. In this case, the dissociation rate obtained here would be an important parameter in determining the upper limit for the DNA repair reaction.

CONCLUSION

By using integrated techniques, we investigated the DNA repair reaction by full-length (6−4) PHR. The integrated techniques allowed us to investigate the local and global dynamics of (6−4) PHR interacting with damaged DNA. We observed a radical intermediate by light excitation of (6−4) PHR. The amount of this radical decreased in the presence of damaged DNA. Because this decrease agreed well with the quantum yield of the restoration of (6−4) PHR, we conclude this decrease reflects the back electron transfer to return the enzyme radical to its original reduced form. This change was not observed within our recording time region. Hence, we conclude that this reaction takes place in the fast time scale (much faster than 50 μs). This fast restoration reaction of (6−4) PHR is similar to that of CPD PHR. The TG signal of (6−4) PHR with damaged DNA is easily distinguishable from that of the enzyme alone or with normal DNA. A significant observation was the rise−decay diffusion signal only in the presence of substrate. We conclude that this *D*-change reaction reflected the dissociation process of the restored DNA from PHR. We determined the time constant for the dissociation reaction to be ∼50 μs. A phase with a similar time constant was also observed in the TA signal, indicating that the observed dissociation reaction involves a conformational change around the FAD chromophore. Rapid dissociation after enzyme restoration would enable this enzyme to seek other damage sites within the enormous contents of DNA and initiate the next restoration more efficiently than other machineries to detect the photoproducts. To our knowledge, this is the first direct observation covering the entire process by a PHR *in vitro*, even though the product releasing process is silent for many spectroscopic tools. The approaches shown here can be applied to the time-resolved detection of the interaction dynamics between biomolecules such as protein−protein or protein−ligand interactions, as well as enzyme−substrate interactions.

ASSOCIATED CONTENT

Supporting Information. Experimental details (section S-1), the principles for the TG and TrL techniques (section S-2),

and supporting results and discussions (sections S-3 and S-4). This material is available free of charge via the Internet at http://pubs.acs.org.

AUTHOR INFORMATION

Corresponding Author
mterazima@kuchem.kyoto-u.ac.jp

ACKNOWLEDGMENT

This work was supported by the Grant-in-Aid for Scientific Research (A) (No. 18205002), Grant-in-Aid for Scientific Research on Innovative Areas (research in a proposed research area) (20107003) from the Ministry of Education, Science, Sports and Culture in Japan (to M.T.), and the National Institutes of Health Grant (GM37684) (to E.D.G.). M.K. was supported by a research fellowship of the Global COE program, International Center for Integrated Research and Advanced Education in Material Science, Kyoto University, Japan. K.H. was supported by The Skaggs Institute for Chemical Biology. We thank Drs. J. A. Tainer and J. L. Tubbs for encouragement and useful discussion.

REFERENCES

(1) Friedberg, E. C.; Walker, G. C.; Siede, W.; Wood, R. D.; Schultz, R. A. *DNA Repair and Mutagenesis*, 2nd ed.; Americal Society for Microbiology; ASM Press: Washington, DC, 2006.
(2) Weber, S. *Biochim. Biophys. Acta* **2005**, *1707*, 1–23.
(3) Sancar, A. *J. Biol. Chem.* **2008**, *283*, 32153–32157.
(4) Sancar, A. *Chem. Rev.* **2003**, *103*, 2203–2238.
(5) Hitomi, K.; DiTacchio, L.; Arvai, A. S.; Yamamoto, J.; Kim, S. T.; Todo, T.; Tainer, J. A.; Iwai, S.; Panda, S.; Getzoff, E. D. *Proc. Natl. Acad. Sci. U.S.A.* **2009**, *106*, 6962–6967.
(6) Hitomi, K.; Kim, S. T.; Iwai, S.; Harima, N.; Todo, T. *J. Biol. Chem.* **1997**, *272*, 32591–32598.
(7) Sancar, G. B.; Jorns, M. S.; Payne, G.; Fluken, D. J.; Rupert, C. S.; Sancar, A. *J. Biol. Chem.* **1987**, *262*, 492–498.
(8) Mees, A.; Klar, T.; Gnau, P.; Hennecke, U.; Eker, A. P.; Carell, T.; Essen, L. O. *Science* **2004**, *306*, 1789–1793.
(9) Aubert, C.; Vos, M. H.; Mathis, P.; Eker, A. P. M.; Brettel, K. *Nature* **2000**, *405*, 586–590.
(10) Kao, Y. T.; Saxena, C.; Wang, L.; Sancar, A.; Zhong, D. *Proc. Natl. Acad. Sci. U.S.A.* **2005**, *102*, 16128–16132.
(11) Maul, M. J.; Barends, T. R. M.; Glas, A. F.; Cryle, M. J.; Domratcheva, T.; Schneider, S.; Schlichting, I.; Carell, T. *Angew. Chem., Int. Ed.* **2008**, *47*, 10076–10080.
(12) Li, J.; Liu, Z.; Tan, C.; Guo, X.; Wang, L.; Sancar, A.; Zhong, D. *Nature* **2010**, *466*, 887–890.
(13) Sadeghian, K.; Bocola, M.; Merz, T.; Schutz, M. *J. Am. Chem. Soc.* **2010**, *132*, 16285–16295.
(14) Mizukoshi, T.; Hitomi, K.; Todo, T.; Iwai, S. *J. Am. Chem. Soc.* **1998**, *120*, 10634–10642.
(15) Hitomi, K.; Nakamura, H.; Kim, S. T.; Mizukoshi, T.; Ishikawa, T.; Iwai, S.; Todo, T. *J. Biol. Chem.* **2001**, *276*, 10103–10109.
(16) Zhao, X.; Liu, J.; Hsu, D. S.; Zhao, S.; Taylor, J.; Sancar, A. *J. Biol. Chem.* **1997**, *272*, 32580–32590.
(17) Glas, A. F.; Schneider, S.; Maul, M. J.; Hennecke, U.; Carell, T. *Chem.-Eur. J.* **2009**, *15*, 10387–10396.
(18) Glas, A. F.; Maul, M. J.; Cryle, M.; Barends, T. R. M.; Schneider, S.; Kaya, E.; Schlichting, I.; Carell, T. *Proc. Natl. Acad. Sci. U.S.A.* **2009**, *106*, 11540–11545.
(19) Domratcheva, T.; Schlichting, I. *J. Am. Chem. Soc.* **2009**, *131*, 17793–17799.
(20) Nakasone, Y.; Eitoku, T.; Matsuoka, D.; Tokutomi, S.; Terazima, M. *J. Mol. Biol.* **2006**, *367*, 432–442.
(21) Eitoku, T.; Zarate, X.; Kozhukh, G. V.; Kim, J.; Song, P.; Terazima, M. *Biophys. J.* **2006**, *91*, 3797–3804.
(22) Tanaka, K.; Nakasone, Y.; Okajima, K.; Ikeuchi, M.; Tokutomi, S.; Terazima, M. *J. Mol. Biol.* **2009**, *386*, 1290–1300.
(23) Nishida, S.; Nada, T.; Terazima, M. *Biophys. J.* **2004**, *87*, 2663–2675.
(24) Inoue, K.; Sasaki, J.; Spudich, J. L.; Terazima, M. *Biophys. J.* **2007**, *92*, 2028–2040.
(25) Nakasone, Y.; Eitoku, T.; Matsuoka, D.; Tokutomi, S.; Terazima, M. *Biophys. J.* **2006**, *91*, 645–653.
(26) Hitomi, K.; Iwai, S.; Tainer, J. A. *DNA Repair* **2007**, *6*, 410–428.
(27) Todo, T.; Kim, S. T.; Hitomi, K.; Otoshi, E.; Inui, T.; Morioka, H.; Kobayashi, H.; Ohtsuka, E.; Toh, H.; Ikenaga, M. *Nucleic Acids Res.* **1997**, *25*, 764–768.
(28) Terazima, M.; Hirota, N. *J. Phys. Chem.* **1992**, *96*, 7147–7150.
(29) Takeshita, K.; Imamoto, Y.; Kataoka, M.; Tokunaga, F.; Terazima, M. *Biochemistry* **2002**, *41*, 3037–3048.
(30) Terazima, M. *Isr. J. Chem.* **1998**, *38*, 143–157.
(31) Terazima, M.; Hirota, N. *J. Chem. Phys.* **1991**, *95*, 6490–6495.
(32) Terazima, M. *Acc. Chem. Res.* **2000**, *33*, 687–694.
(33) Muller, F.; Brustlein, M.; Hemmerich, P.; Massey, V.; Walker, W. H. *Eur. J. Biochem.* **1972**, *25*, 573–580.
(34) Sober, H. A. *CRC Handbook of Biochemistry Selected Data for Molecular Biology*; Chemical Rubber Co.: Cleveland, OH, 1968; pp C-30−C-35.
(35) Espange, A.; Byrdin, M.; Eker, A. P. M.; Brettel, K. *ChemBioChem* **2009**, *10*, 1777–1780.